Adsorption 9: 295–302, 2003

Mechanisms of Molecular Mobility of Oxygen and Nitrogen in Carbon Molecular Sieves*

DONGMIN SHEN
DataXplore, Inc., 38 Snyder Avenue, Berkeley Heights, NJ 07922, USA

MARTIN BÜLOW†
BOC Process Gas Solutions Technology, 100 Mountain Avenue, Murray Hill, NJ 07974, USA
martin.bulow@boc.com

NORBERTO O. LEMCOFF
United Technologies Research Center, 411 Silver Lane, East Hartford, CT 06108, USA

Received June 3, 2002; Revised March 28, 2003; Accepted May 12, 2003

Abstract. Molecular mobility of oxygen, O_2, and nitrogen, N_2, in Carbon Molecular Sieves, CMS, was investigated using the Frequency Response, FR, technique to identify mass-transfer mechanisms and related kinetic time constants. The FR data showed that O_2 mobility in four types of CMS was dominantly controlled by surmounting surface-barrier resistances, whereas the mobility of both O_2 and N_2 in pellets of a fifth CMS type obeyed the *Fickian* diffusion model. Temperature and pressure dependences of surface-barrier penetration time constants were obtained for O_2 and N_2 in several of those CMS materials. The kinetic time constants of surface-barrier penetration were related to *Langmuir*-type rate constants, which indicates that kinetic behavior of O_2 therein could also be interpreted in terms of a *Langmuir*-kinetics equation.

Keywords: oxygen, nitrogen, carbon molecular sieve, sorption, molecular mobility, surface barrier, *Langmuir* kinetics, frequency response technique, piezometric technique

1. Introduction

Pressure-swing adsorption, PSA, processes for separation of gas mixtures may be governed by both equilibrium and non-equilibrium sorption mechanisms or dominantly by one of them. Non-equilibrium processes are particularly challenging, since sorption-kinetic separations may be quite different from those under equilibrium conditions. Air separation for N_2 production using CMS is an industrially important example of such a kinetically controlled process (Pilarczyk and Knoblauch, 1988; Schröter, 1993; Lemcoff, 1998). Different CMS sorbents may vary sufficiently in their micropore structure, which leads to a variety of applications, cf., Pilarczyk and Knoblauch (1988), as well as to differences in sorption-uptake mechanisms and, thus, in kinetic models for an appropriate description of sorption-separation processes. Transport of N_2 and O_2 in CMS sorbents obeys either surmounting a surface-barrier resistance confined at the micropore entrances (LaCava et al., 1989; Fitch et al., 1994; Srinivasan et al., 1995; Sircar et al., 1997; Farooq et al., 1999; Sundaram et al., 2001), or a diffusional process within the micropores (Ruthven et al., 1992; Srinivasan et al., 1995;

*This paper had been presented in part at the AIChE 2001 Annual Meeting, Reno, NV, Nov. 4–10, 2001.
†To whom correspondence should be addressed.

Farooq et al., 1999; Sundaram et al., 2001) or a superposition of both (Loughlin et al., 1993). The particular mechanism depends on relative sizes of effective cross-sections of micropore openings, which may vary to some extent, and molecules of sorbing species (Bülow, 1985; Pilarczyk and Knoblauch, 1987). Therefore, it is important to know details of sorption kinetics associated with each individual of such materials for optimizing and modeling PSA processes, for the specific purposes of their usage.

The FR technique has been proven to be a prominent technique for studies of molecular mobility in both microporous and bidisperse porous sorbent structures (Yasuda, 1976, 1982, 1991; Jordi and Do, 1993; Sun and Bourdin, 1993; Shen and Rees, 1994; Sun et al., 1994; Yasuda, 1994). This method is also capable of describing qualitatively and quantitatively *Fickian* diffusion and surface-barrier penetration or analyzing both resistances if they occur simultaneously (Yasuda, 1976, 1982; Jordi and Do, 1993; Shen and Rees, 1994; Yasuda, 1994), which holds for other methods as well, cf., Bülow (1991) and Bülow and Micke (1995). In the current paper, the FR technique is used to study molecular mobility of O_2 and N_2 in various CMS sorbents, to qualitatively identify transport mechanisms and to quantitatively determine the time constants associated with those mechanisms.

2. Experimental

2.1. Frequency-Response Technique

Many FR models have been developed and utilized for a study of molecular transport in monodisperse micropore and bidisperse micro/macropore systems (Jordi and Do, 1993; Sun and Bourdin, 1993; Sun et al., 1994; Yasuda, 1994). By thoughtful design of FR experiments, one can identify the type of transport resistance, which controls the mass-transfer process and determines the corresponding time constants. For CMS particles, at least three major mass-transfer resistances, which may possibly occur simultaneously during sorption uptake or release, have to be considered: (i) intraparticle meso/macropore diffusion, (ii) surface-barrier penetration, and (iii) intraparticle micropore diffusion. In principle, sorption-heat generation and release may affect each of these mass-transfer mechanisms, and they need be analyzed, in addition, if mass and heat transfer proceed at comparable rates.

The FR model to *Fick*'s second diffusion law of a single component in an isotropic sphere that is subjected to a periodic, sinusoidal surface-concentration modulation, is outlined as follows (Yasuda, 1991, 1994):

$$\text{In-phase:}\quad (p_B/p_S)\cos(\phi_S - \phi_B) - 1 = K_{fr}\delta_{in}, \tag{1}$$

$$\text{Out-of-phase:}\quad (p_B/p_S)\sin(\phi_S - \phi_B) = K_{fr}\delta_{out}, \tag{2}$$

where K_{fr} is an equilibrium constant associated with the sorption-isotherm slope at the equilibrium pressure of the FR experiment. In the FR apparatus used for this study, square-wave forms of volume modulations are utilized. The FR parameters are derived for the equivalent fundamental sine-wave perturbation by using a *Fourier* transformation of the pressure square-wave forms. As a result, a phase-angle difference, $\phi_S - \phi_B$, is obtained, where ϕ_S and ϕ_B are the phase angles of the pressure-response curves measured in presence and absence of sorbent, respectively. The pressure-amplitude ratio, p_B/p_S, is also determined, where p_B and p_S are the amplitudes of the pressure responses to volume perturbation in absence and presence of sorbent, respectively.

The characteristic functions of FR models for three possible cases of mass-transfer resistance, i.e., diffusion, surface barrier, and the complex of both, are given as follows (Yasuda, 1991; Sun and Bourdin, 1993; Yasuda, 1994):

$$\delta_{in}(\eta, t_s, \omega) = \frac{\delta_{in}(\eta, \omega)}{(1 + \delta_{out}(\eta, \omega)\omega t_s)^2 + (\delta_{in}(\eta, \omega)\omega t_s)^2}, \tag{3}$$

$$\delta_{out}(\eta, t_s, \omega) = \frac{\delta_{out}(\eta, \omega) + (\delta_{in}(\eta, \omega)^2 + \delta_{out}(\eta, \omega)^2)\omega t_s}{(1 + \delta_{out}(\eta, \omega)\omega t_s)^2 + (\delta_{in}(\eta, \omega)\omega t_s)^2}. \tag{4}$$

Equations (3) and (4) reduce to the case of a pure diffusional process if $t_s = 0$, or to the case of pure surface-barrier penetration if $t_d = 0$. If the time constants $t_s$and t_d are close to each other, both diffusion and surmounting surface-barrier resistances may control the sorption kinetics.

Figure 1 demonstrates the influence of the time constants for micropore diffusion, t_d, and surface-barrier penetration, t_s, on the FR curves. For $t_d/t_s > 1000$, the FR curves coincide with the ones for a pure diffusion-controlled process, indicating that the mass-transfer process is controlled dominantly by micropore diffusion. On the other hand, if the ratio t_d/t_s is close to 1, the

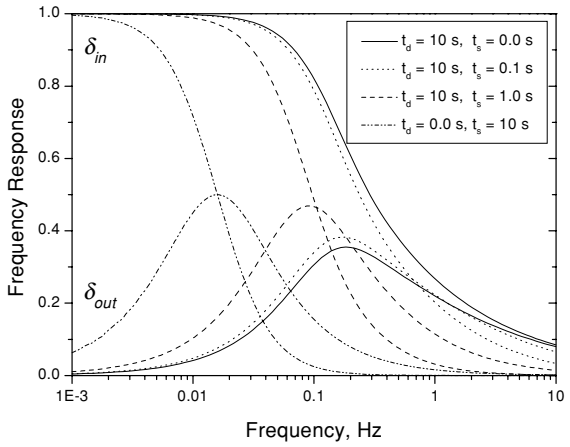

Figure 1. FR curves for surface-barrier penetration, $t_d = 0$; micropore diffusion, $t_s = 0$; and combined processes, calculated by Eqs. (3) and (4) with $K_{\text{fr}} = 1.0$ and time constants indicated.

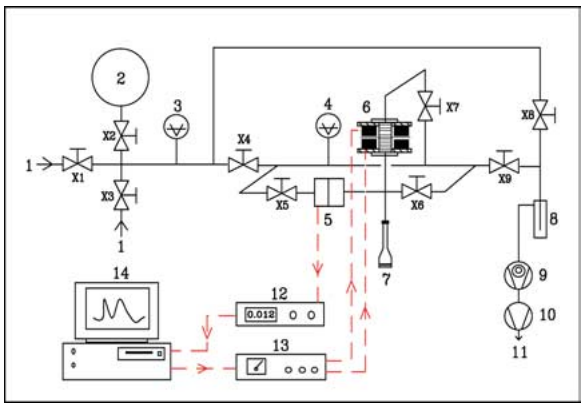

Figure 2. Scheme of the frequency-response apparatus. X1–X9: vacuum valves; 1, 2: gas inlets; 2: gas storage; 3, 4: absolute-pressure Baratron sensors; 5: differential-pressure Baratron sensor; 6: electromagnetic volume-modulation unit; 7: sorbent-sample holder; 8: cold trap; 9: turbo-molecular pump; 10: rotary pump; 11: vent; 12: pressure-display unit; 13: electromagnetic drive unit; and 14: PC with fast data-acquisition interface.

FR curves are very close to those for a dominant penetration of surface-barrier resistances, indicating that this process becomes the rate-limiting mass-transfer process. If the ratio t_d/t_s is in between those numbers, for example, between 10 and 100, the FR curves are determined by both diffusional and surface-barrier penetration time constants.

2.2. *Frequency-Response Experiments*

The frequency-response apparatus used for this study was built at BOC, Murray Hill, NJ. Principal features of the system are shown schematically in Fig. 2.

In the FR method, a dose of sorbate is brought into sorption equilibrium with the sorbent. A square-wave modulation of ca. $\pm$ 1% is then applied to the gas-phase equilibrium volume, V_e, which is the volume between the parts 5, 6, X6 and 7, cf., Fig. 2. The FR software controls and runs automatically the FR experiments by scanning frequencies in a range, (0.001–10) Hz, over certain increments. The modulation is activated by applying a current to each of the two electromagnets of an in-house made volume-modulation unit, which in turn moves rapidly the disc between the electromagnets to the respective energized electromagnet. The stainless-steel bellows attached to the disc, which is part of the gas-phase volume, is expanded or contracted to cause a change of volume, V_e, of ca. $\pm$ 1%. The frequency range mentioned is scanned over 30 increments. Rate constants, which can be covered by this approach, are within bounds of 0.01 to 1000 seconds. The range of diffusivities measurable depends on the sorbent-particle size. The pressure response to the volume change is measured with a high-accuracy differential MKS-Baratron pressure transducer, type 699A (10 torr). The volume, V_e, of the sorption chamber in the actual FR system amounts to ca. 120 cm^3.

The frequency is computer-controlled through a data-acquisition interface (model AT-MIO-16X, National Instruments, USA) that is also used to collect the pressure data from the Baratron transducer. The conversion rate of the ADC in the interface unit must be high enough to cope with fast data acquisition at 10 Hz and a few milliseconds of pressure-transducer response time. The quality of *Fourier* transformations of the pressure data is excellent even at 10 Hz. High-harmonic *Fourier* transformations can be applied to extend the frequency range up to 100 Hz to follow even fast transport processes.

Prior to FR experiments, CMS sample is activated by heating in vacuo from ambient temperature to 350°C over a 3 hr period, and then maintained at 350°C for another 3 hr at pressure, $<10^{-4}$ torr. After activation, the sample is cooled to the experimental temperature and kept at it during subsequent FR measurements with an accuracy of ca. $\pm$ 0.2°C. The sorbate is admitted to the activated sample and allowed to equilibrate towards P_e, which is controlled with a high-accuracy absolute MKS-Baratron pressure transducer, type 615A, (100 torr), at the temperature of experimental runs. The electromagnets are activated at starting frequency, i.e.,

Table 1. CMS adsorbents used.

Adsorbent	Shape	Size (mm)	Effective pore size (nm)
CMS-6	Pellets	~2 × 2	~0.4
CMS-8	Pellets	~2 × 2	~0.9
CMS-8B	Beads	0.24 × 0.5	~0.9
CMS-11	Pellets	~2 × 2	~0.4
CMS-11B	Beads	0.17 × 0.24	~0.4
CMS-20	Pellets	~2 × 2	~0.4
MSC3K-183	Pellets	~2 × 2	>0.4

0.01 or 10 Hz, and the pressure response is recorded over five cycles after periodic steady state had been established, i.e., after the cycling time exceeded the kinetic time constant. The pressure response to the volume change over the whole frequency range is measured in presence and absence of sorbent to obtain the difference of the respective FR parameters. The FR parameters measured are fitted with appropriate models using least-square fitting routines to obtain the best fitting parameters, e.g., t_d, t_s, and $K_{\rm fr}$.

2.3. *Carbon Molecular Sieves*

Five CMS samples, CMS-06, CMS-08, CMS-11, CMS-20, and MSC3K183, of different origin, were investigated with regard to molecular mobility of O_2 and N_2 in their sorption states. The CMS samples available in shapes of cylindrical pellets of 2 mm in diameter were cut to a length of ca. 2 mm, so that the resulting particles could approximately be assumed to be spheroid, for data analysis. In addition, CMS-08 and CMS-11 pellets were crushed into small "beads" of sizes, (0.24 × 0.50) mm and (0.17 × 0.24) mm, named CMS-08B and CMS-11B, respectively. The effective micropore openings of CMS-06, CMS-11 and CMS-20 are ca. 0.4 nm; those of MSC3K183 are >0.4 nm; and those of CMS-08 are ca. 0.9 nm, cf., Table 1. In FR measurements, (1–1.5) g of each CMS sample was used.

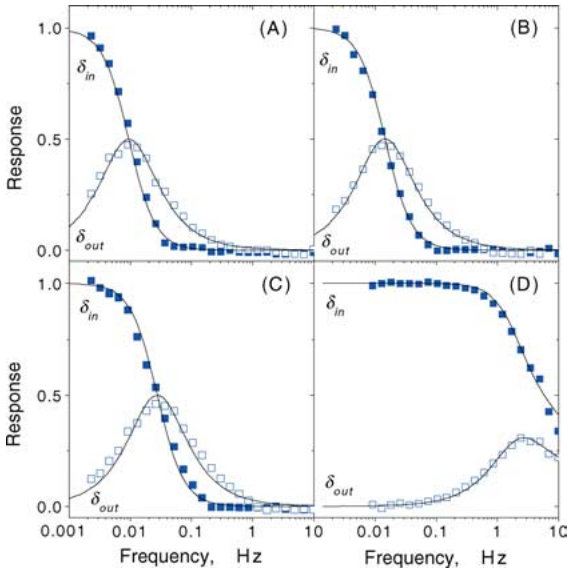

Figure 3. FR curves of O_2 mobility in CMS-11 (A), CMS-06 (B), CMS-20 (C) and CMS-08 (D) pellets at 20°C and 20 torr of equilibrium pressure. Solid curves are fitted by FR models with parameters given in Table 2.

The gases used in the FR measurements were supplied by BOC Gases, each with a purity of 99.999%.

3. Results and Discussion

FR curves for O_2 in all five CMS-pellet samples were measured at several temperatures, (0 to 60)°C, and equilibrium pressures, (2 to 40) torr. Figure 3 shows the FR curves for CMS-06, CMS-11, CMS-20 and CMS-08 at 20°C and 20 torr.

The curves for the first three sorbents are characteristic of a surface barrier-controlled mass-transfer process, whereas those for CMS-08 have the profile of a diffusional transport. The experimental data for CMS-06, CMS-11 and CMS-20 can be reproduced by the surface-barrier model with parameters listed in Table 2.

Table 2. FR models and parameters used in Figs. 3, 5 and 6.

	CMS-11	CMS-06	CMS-20	CMS-08	CMS-08	MSC3K183	MSC3K183
Gas	O_2	O_2	O_2	O_2	N_2	O_2	N_2
Mode	Surface barrier	Surface barrier	Surface barrier	Diffusion	Diffusion	Surface barrier	Surface barrier
t_s (s)	16.85	11.36	5.75	0	0	2.45	60.00
t_d (s)	0	0	0	0.687	0.872	0	0
$K_{\rm fr}$ (g^{-1})	0.079	0.061	0.065	0.058	0.063	0.065	0.072

The time constants that determine the position of the FR curves, indicate a sequence of mass-transfer rates, CMS-08 > CMS-20 > CMS-06 > CMS-11, irrespective of the type of mass-transfer mechanism that controls the sorption process.

It was reported (Jüntgen et al., 1974; Cabrera et al., 1993; Armor, 1994; Coe, 1997) that for CMS pellets with "ink-bottle"-type micropores, the kinetic selectivity of O_2 over N_2 was maintained on crushed "bead" particles if the size of the crushed "beads" was larger than $\sim$100 μm, but the selectivity was reduced if the "bead" sizes became $<$100 μm. It was suggested that those micropore systems of the original CMS pellets were not damaged, and the mass-transfer mechanism was not changed if the particles were crushed to a certain extent, e.g., $>$100 μm. This is because the surface-barrier resistance is mostly confined in the regions of micropore openings of CMS pellets and, therefore, should not depend on either their size or shape, as long as the microparticle is not damaged. To prove whether surface-barrier penetration remains to be the mass transfer-controlling step in crushed CMS particles, CMS-11B "beads" of size, $>$170 μm, were tested under identical experimental conditions. The FR curves of O_2 in these small "beads" are similar to those in the original CMS-11 pellets, and they can also be reproduced by a surface-barrier model with the parameters, $t_s = 26.72$ s and $K_{\mathrm{fr}} = 0.072$ g^{-1}. Both similarity between FR curves and closeness of FR parameters obtained for O_2 in these two CMS-11 and CMS-11B samples of different size, confirm that the rate of surface-barrier penetration by O_2 dominates its uptake by these materials; and the transport resistance is at the pore openings of the microparticulate domains that form the CMS pellets.

Unlike the materials CMS-06, CMS-11 and CMS-20, which exhibit unique characteristics for a surface barrier-controlled mass-transfer process, sorption kinetics of both O_2 and N_2 in CMS-08 pellets are controlled dominantly by diffusional resistances, cf., Jüntgen (1975) and Pilarczyk and Knoblauch (1987). A different mass-transfer mechanism is expected for CMS-08 since the effective cross-section of micropore openings of this sorbent amounts to ca. 0.9 nm, which is much larger than the corresponding values for the other materials. Figure 4 shows that the FR data for both O_2 and N_2 in CMS-08 pellets can be fitted by the *Fickian* diffusion model, with the parameters given in Table 2.

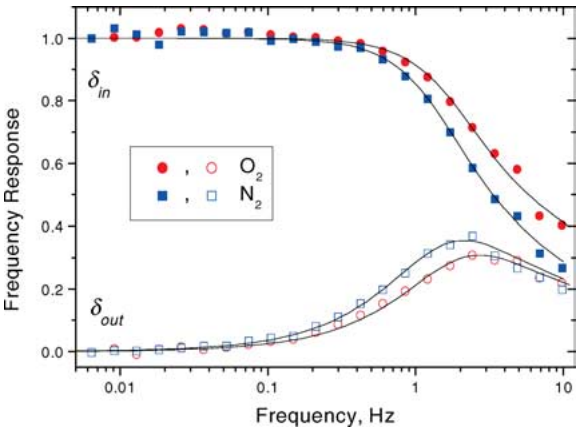

Figure 4. FR curves of O_2 and N_2 mobility in CMS-08 pellets at 20°C and 20 torr of equilibrium pressure. Solid curves are fitted by the diffusion model with $t = 0.687$ s and $K_{\mathrm{fr}} = 0.058$ g^{-1} for O_2, and $t = 0.872$ s and $K_{\mathrm{fr}} = 0.063$ g^{-1} for N_2.

These data also show that molecular mobility of O_2 in CMS-08 is only slightly higher than that of N_2, and, therefore, this sorbent does not exhibit kinetic selectivity for O_2 over N_2. Although the experimental points can be reproduced by the diffusion model, it cannot be decided without further tests whether the diffusional process is controlled by diffusion in micropores, macropores, or in both, simultaneously. If the sorption process would have been controlled by an intraparticle (micropore) diffusional resistance, the FR curves should not depend on pellet size, but on both size and shape of the microparticulate domains that form the CMS macroparticle. On the other hand, if the sorption rates were controlled by an interparticle transport (i.e., in pores between microparticulate domains) such as transport process in meso- and/or macropores, the FR curves should depend on size and shape of the pellets but not on those of the microparticulate domains, and they should appear at different frequencies for differently sized macroparticles.

Compared with the corresponding curves found for pellets, the FR curves of O_2 and N_2 measured on crushed CMS-08B "beads" of average size, (0.24 $\times$ 0.50) mm, appear at high frequencies, cf., Fig. 5.

This indicates that the diffusional time constants depend on sorbent-pellet size, which proves that the mobility of O_2 and N_2 in CMS-08 pellets is mostly controlled by surmounting macropore resistances rather than by those in micropores.

The FR curves of N_2 in CMS-6, CMS-11, CMS-11B and CMS-20 were apparently flat and close to

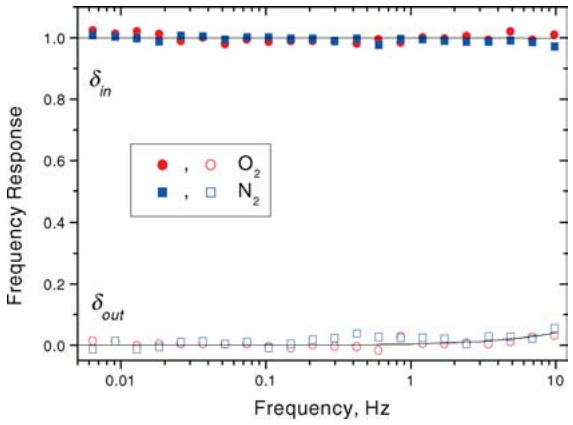

Figure 5. FR curves of O_2 and N_2 mobility in CMS-08B beads at 20°C and 20 torr of equilibrium pressure. Solid curves are fitted by the diffusion model with $t < 0.01$ s, $K_{fr} = 0.053$ g^{-1} for O_2, and $t < 0.01$ s and $K_{fr} = 0.054$ g^{-1} for N_2.

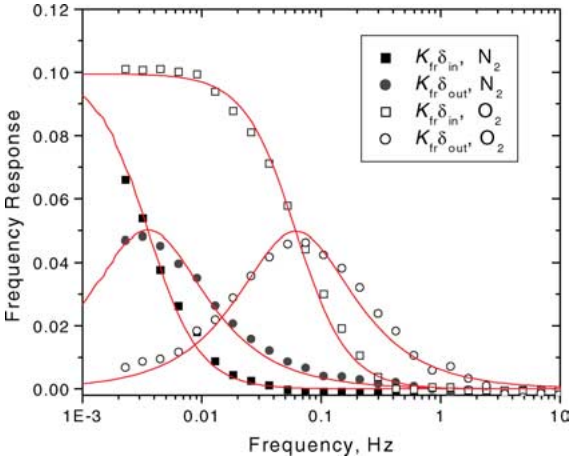

Figure 6. FR curves of O_2 and N_2 mobility in MSC3K183 pellets at 20°C and 20 torr of equilibrium pressure. Solid curves are fitted by the surface-barrier model with $t_s = 2.45$ s, $K_{fr} = 0.065$ g^{-1} for O_2, and $t_s = 60.0$ s and $K_{fr} = 0.072$ g^{-1} for N_2.

zero at experimental temperatures chosen, which suggests much slower kinetic processes for N_2 in these CMS samples than those for O_2 at given conditions. On MSC3K183, which is a CMS material with somewhat larger effective pore sizes, the FR curves for mobility of both O_2 and N_2 appeared at higher frequencies, as shown in Fig. 6, but still being characteristic of a process controlled by surface-barrier penetration. These curves could be fitted by the surface-barrier resistance model with the parameters listed in Table 2.

The surface-barrier time constants indicate that molecular mobility and, hence, uptake of N_2 by MSC3K183 is by a factor of ca. 24 slower that that of O_2, at 20°C and 20 torr.

Temperature dependences of time constants for surface-barrier penetration by O_2 in CMS-06 and CMS-20, and by O_2 and N_2 in MSC3K183 pellets were obtained over a range, (0 to 60)°C, and at an equilibrium pressure, 20 torr.

The surface-barrier penetration time constant, t_s, and sorption-equilibrium parameter, K_{fr}, determined by fitting the experimental data points to the surface-barrier model, are listed in Table 3, together with the theoretical equilibrium constants, K_{iso}, calculated from sorption isotherms measured independently on the same CMS-06 sample using a piezometric technique (Bülow et al., 1986). The ratios of experimental and theoretical equilibrium constants are close to unity, which suggests that all sorbing species were detected within the frequency "window", and a correct model was applied to reproduce the experimental data. The low value obtained for CMS-06 at 273 K may be due to experimental errors.

Values of activation energy, E_a, for the penetration of surface barriers were calculated from the temperature dependences of the reciprocal time constants. Figure 7 shows such dependences for O_2 and N_2 mobility in pellets of the sorbents CMS-06, CMS-20 and MSC3K183.

The surface-barrier resistance to O_2 mobility decreases according to the sequence, CMS-06 > CMS-20 > MSC3K183. However, the activation energies are very close to each other, viz., ca. 21.3, 21.5 and 21.6 kJ/mol, respectively. These values are larger

Table 3. FR data of O_2 and N_2 in CMS-06, CMS-20 and MSC3K183 as obtained at 20 torr.

	CMS-06 (O_2)				CMS-20 (O_2)		MSC3K183 (O_2)		MSC3K183 (N_2)	
T (K)	t_s (s)	K_{fr} (g^{-1})	K_{iso} (g^{-1})	K_{fr}/K_{iso}	t_s (s)	K_{fr} (g^{-1})	t_s (s)	K_{fr} (g^{-1})	t_s (s)	K_{fr} (g^{-1})
273	16.60	0.064	0.103	0.62	10.44	0.106	4.95	0.118	90.92	0.092
293	11.36	0.061	0.060	1.02	5.75	0.065	2.45	0.068	60.00	0.072
313	5.72	0.040	0.038	1.05	2.92	0.044	1.25	0.045	25.40	0.050
333	3.10	0.027	0.026	1.04	1.97	0.031	0.95	0.029	9.57	0.032

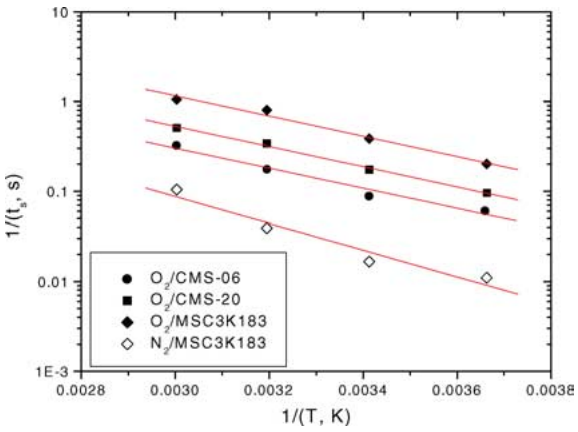

Figure 7. Temperature dependence of reciprocal time constants of surface-barrier penetration in CMS-06 (●), CMS-20 (■) and MSC3K183 (◆) for O_2 mobility at 20 torr, and MSC3K183 (◇) for N_2 mobility at 20 torr.

than 19.6 kJ/mol, which was reported by Jüntgen et al. (1974) assuming a diffusional process to be dominant in their CMS. The activation energy for N_2 in MSC3K183 amounts to ca. 28.4 kJ/mol.

The value of activation energy for surmounting surface-barrier resistances by O_2 molecules is close to that of their sorption heat, e.g., on CMS-06, which amounts to ca. 22.8 kJ/mol, as calculated from sorption isotherms on the same sample. Such a closeness between the activation energy for the process of surface-barrier penetration, and the sorption heat may suggest a mass-transfer control in accordance with the *Langmuir*-kinetics equation as described by Dominguez et al. (1988). If a sorption-kinetic behavior obeys the *Langmuir*-kinetics equation, the time constant, t_s, of surface-barrier penetration may be related to the rate constants for adsorption, k_a, and desorption, k_d, as follows (Yasuda, 1976):

$$1/t_s = k_a p_e + k_d. \tag{5}$$

To test this equation, the molecular mobility of O_2 in CMS-06 pellets was measured as a function of equilibrium pressure. In the experimental pressure range, (5 to 40) torr, at a temperature of 20°C, the FR curves measured were all characteristic of a dominant surface-barrier penetration of the mass transfer in this CMS material.

Figure 8 shows the pressure dependence of the reciprocal surface-barrier time constants obtained for O_2 on CMS-06 pellets, and Table 4 lists the FR sorption-equilibrium constants, K_{fr}, measured and, K_{iso}, calculated from sorption isotherms. A fit of constants of Eq. (5) to those data points, as shown in Fig. 8, yields the values, $k_a = 3.72\,\text{E-}5\ \text{s}^{-1}\ \text{torr}^{-1}$ and $k_d = 8.73\,\text{E-}2\ \text{s}^{-1}$. From these values a *Langmuir* sorption-equilibrium constant, 4.26 E-4 torr^{-1}, is obtained. This *Langmuir* constant agrees reasonably well with the corresponding one, viz., 3.28 E-4 torr^{-1}, as calculated from the O_2-sorption isotherm on the same sorbent at the same temperature, 20°C. This agreement indicates that the *Langmuir*-kinetics model could indeed be used to describe the sorption-kinetic behavior for a series of CMS pellets, and as reported previously (Dominguez et al., 1988; LaCava et al., 1989; Loughlin et al., 1993) in order to predict mass transfer of O_2 and N_2 in carbon molecular sieve sorbents.

Table 4. FR data for O_2 on CMS-06 measured at 20°C.

P_e (torr)	t_s (s)	K_{fr} (g^{-1})	K_{iso} (g^{-1})	K_{fr}/K_{iso}
5	11.44	0.066	0.061	1.08
10	11.41	0.062	0.061	1.02
20	11.36	0.061	0.060	1.02
40	11.27	0.059	0.060	0.98

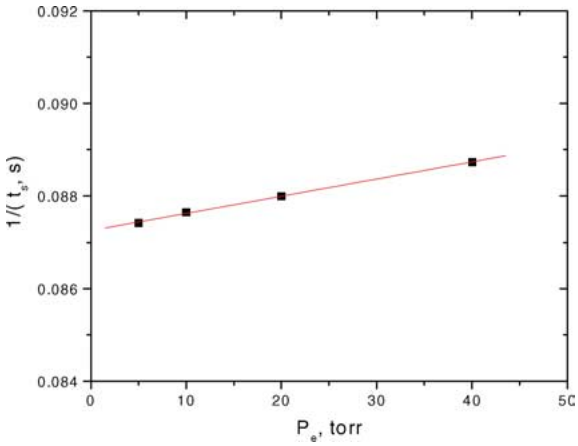

Figure 8. Pressure dependence of reciprocal time constants of surface-barrier penetration for O_2 uptake by CMS-06 pellets at 20°C. Solid line is fitted by Eq. (5) with $k_a = 3.72\text{E-}5\ \text{s}^{-1}\ \text{torr}^{-1}$ and $k_d = 8.73\text{E-}2\ \text{s}^{-1}$.

4. Conclusions

The FR technique is a prominent tool to study molecular mobility of O_2 and N_2 in CMS pellets and beads to identify mass-transfer mechanisms. Results of its

application show that O_2 mobility in CMS-06, CMS-20, CMS-11 and MSC3K183 samples is governed dominantly by surmounting surface barriers where the resistances are located at the micropore entrances within the microparticulate domains that form the CMS pellets. In MSC3K183 pellets with larger effective pore openings, the FR curves for both O_2 and N_2 were measured, and they were both controlled dominantly by surface barrier resistances. The uptake of O_2 in MSC3K183 is quicker than that of N_2 by a factor of ca. 24 at 20°C and 20 torr.

Temperature dependences of surface-barrier time constants for O_2 in CMS-06 and CMS-20 and for O_2 and N_2 in MSC3K183 were obtained. The pressure dependence of the kinetic time constants for surface-barrier penetrations obtained for O_2 in CMS-06 could be related to *Langmuir*-type rate constants. This indicates that the kinetic behavior could as well be described by a *Langmuir*-kinetics equation, in agreement with previous literature reports.

For CMS-08, the FR data show a mass-transfer mechanism for both O_2 and N_2, which obeys the *Fickian* diffusion model, with a mass-transfer rate for O_2 slightly higher than that for N_2. This finding is in agreement with the comparatively large average cross-section of micropore openings of the latter CMS.

Acknowledgments

The authors thank Dr. F.R. Fitch, Murray Hill, USA, for helpful discussions of sorption properties of CMS materials. They also express their gratitude to Dr. H.-J. Schröter, CarboTech, Essen, Germany, for the supply of several materials used, and inspirational conversations on manufacture and properties of CMS.

References

Armor, J.N., in *Separation Technology*, E.F. Vansant (Ed.), pp. 163–199, Elsevier, Amsterdam, 1994.

Bülow, M., *Z. Chem. (Leipzig)*, **25**, 81–89 (1985).

Bülow, M., P. Struve, and W. Mietk, *Z. Physik. Chem. (Leipzig)*, **267**, 613–617 (1986).

Bülow, M., *Stud. Surf. Sci. Catalysis*, **60**, 199–212 (1991).

Bülow, M. and A. Micke, *Adsorption*, **1**, 29–48 (1995).

Cabrera, A.I., J.E. Zehner, C.G. Coe, T.R. Gaffney, T.S. Farris, and J.N. Armor, *Carbon*, **31**, 969–976 (1993).

Coe, C.G., in *2nd Topical Conf. Separation Sci. Technol*., pp.1272–1277, AIChE 1997 Annual Meeting, Los Angeles, November 17–19, 1997.

Dominguez, J.A., D. Psaras, and A.I. LaCava, *AIChE Symp. Ser*., **84**(264), 73–82 (1988).

Farooq, S., R. Gupta, and J. Ambalavanan, in *4th Topical Conf. Separation Sci. Technol*., AIChE 1999 Annual Meeting, Dallas, Oct. 31–Nov. 5, 1999.

Fitch, F.R., M. Bülow, and A.I. LaCava, *Gas Sep. Purif*., **8**, 45–51 (1994).

Jordi, R.G. and D.D. Do, *Chem. Eng. Sci*., **48**, 1103–1130 (1993).

Jüntgen, H., K. Knoblauch, H. Münzner, H.-J. Schröter, and D. Zündorf, in *4th Internat. Carbon Graphite Conf.*, p. 139, London, Sept. 23–27, 1974.

Jüntgen, H., *Ber. Bunsen-Gesellschaft Physik. Chem.*, **79**, 747–748 (1975).

LaCava, A.L., V.A. Koss, and D. Wickens, *Gas Sep. Purif*., **3**, 180–186 (1989).

Lemcoff, N.O., *Stud. Surf. Sci. Catalysis*, **120**, 347–374 (1998).

Loughlin, K.F., M.M. Hassan, A.I. Fatehi, and M. Zahur, *Gas Sep. Purif*., **7**, 264–273 (1993).

Pilarczyk, E. and K. Knoblauch, in *Separation Technology*, N.N. Li and H. Strathmann (Eds.), pp. 522–550; in *Proc. Engng. Foundation Conf., Schloß Elmau*, Germany, April 27–May 1, 1987, United Engng, Trustees, NewYork, 1988.

Ruthven, D.M., Z. Xu., and S. Farooq, *Chem. Eng. Sci*., **47**, 4305–4308 (1992).

Schröter, H.-J., *Gas Sep. Purif*., **7**, 247–251 (1993).

Shen, D. and L.V.C. Rees, *J. Chem. Soc. Faraday Trans*., **90**, 3017–3022 (1994).

Sircar, S., R.M. Rynders, and M.B. Rao, *AIChE J.*, **43**, 2456–2470 (1997).

Srinivasan, R., S.R. Auvil, and J.M. Schork, *Chem. Eng. J.,* **57**, 137–144 (1995).

Sun, L.M. and V. Bourdin, *Chem. Eng. Sci*., **48**, 3783–3793 (1993).

Sun, L.M., F. Meunier, Ph. Grenier, and D.M. Ruthven, *Chem. Eng. Sci*., **49**, 373–381 (1994).

Sundaram, S.M., H. Qinglin, and S. Farooq, in *Fundamentals of Adsorption 7*, K. Kaneko, H. Kanoh, and Y. Hanzawa (Eds.), pp. 779–786; in *Proc. 7th International Conference on Fundamentals of Adsorption*, Nagasaki, May 20–25, 2001, International Adsorption Society, IK International, Ltd., 2002.

Yasuda, Y., *J. Phys. Chem*., **80**, 1867–1871 (1976).

Yasuda, Y., *J. Phys. Chem*., **86**, 1913–1917 (1982).

Yasuda, Y., *Bull. Chem. Soc. Jpn*., **64**, 954–961 (1991).

Yasuda, Y., *Heterogen. Chem. Rev.,* **1**, 103–124 (1994).